Scientific Journal for Damietta Faculty of Science **14**(2) 2024, 13-23
doi: 10.21608/SJDFS.2024.289628.1168
ISSN Print 2314-8594
ISSN Online 2314-8616

https://sjdfs.journals.ekb.eg/

Study of Photodegradation of Dianix Blue Dye for Commercial Industrial Wastewater in the Presence of Zeolite-TQD

Waleed M. Saad[1], Farid Sh. Mohamed[1], Ashraf A. El-Bindary[1] and Walied A.A. Mohamed[*2]

[1]Chemistry Department, Faculty of Science, Damietta University, Damietta 34517, Egypt.
[2]Inorganic Chemistry Department, National Research Centre, Dokki, Giza, Egypt.

Received: 14 May 2024 /Accepted: 03 June 2024

[*]Corresponding author's E-mail: el3shry73@gmail.com

Abstract

Pollutant removal is critical, as evidenced by the need for clean water, the rise in industrial effluent, and environmental pollution. One very efficient way to get rid of impurities from water and industrial effluent is to use zeolite removal. TiO_2 is one of the special photophysical characteristics of zeolite, which is distinguished by its numerous microscopic pores, high absorption capacity, and thermochemical stability. Sol-gel was used to synthesise zeolite and TiO_2 quantum dots (TQD) with diameters ranging from 307 to 48 nanometers. In this work, zeolite microparticles were treated with TiO_2 nanoparticles. The zeolite/TiO_2 composites were assessed using SEM, diffuse reflectance spectroscopy, Brunauer-Emmett-Teller, and X-ray diffractometer investigations. The results showed that the presence of TiO_2 nanoparticles reduces the specific surface area. However, it results in the ability to absorb ultraviolet rays. Increasing the amount of TiO_2 will cause the absorption edge to move. The photocatalytic properties of the compounds were evaluated using Blue Dianix dye removal analysis. Zeolite-TQD, with a specific surface area of 292.39 m^2/g and a band gap energy of 3.57 eV, is the most effective material. Evidence of enhanced photocatalytic performance was obtained through analysis of spent chemical oxygen. We also confirmed the photodegradation rate of real industrial effluents using COD limitations specified in the Egyptian Environmental Law. Nine recycled zeolite-TQD samples were examined using COD measurements.

Keywords: Blue Dianix dye, modified precipitation technique, Zeolite -TQD, and COD analysis.

Introduction

The dye is widely used in textiles, printing, food coloring and dyeing in today's industrial civilization. The amount of dye lost during dyeing processes and discharged into wastewater is estimated to range between 1 and 15%. Disposal of industrial waste is critical because the release of strongly colored wastewater into the environment causes aesthetic pollution (even a little dye is noticeable) and disturbs aquatic life, among other environmental problems. In other words, dyes pose a significant risk to the aquatic environment.(Lanjwani M.F., 2024) However,

color pollution has an impact on health as well as water quality because some dyes are carcinogenic and mutagenic. Consequently, throughout the previous 20 years, research has been done to create methods for eliminating, destroying, or recovering colours that are present in water. The target pollutant in this investigation was indigo dye, which was subjected to photodegradation. Indigo dye is a member of the pot dyes (Joksimovic K,2022), an archaic category of colours. These days, it is manufactured industrially in huge amounts (20 million kg per year), mostly for the purpose of dying cotton fabrics like denim or jeans (Ahsan, M.A. et al., 2023). The organic dye indigo has the chemical formula $C_{16}H_{10}N_2O_2$. This dye is an indigo-derived blue colourant. Semiconductors are used in photocatalysis, an improved oxidation process.Using such TiO_2 as photocatalysts is a viable on-site method of removing organic contaminants from water (Irirerkratana.K, 2019). When an activated photocatalyst 4 is present, photocatalysis is a heterogeneous catalytic reaction that occurs under UV light irradiation. Numerous research on the use of titanium dioxide in the photodegradation of organic dyes in wastewater have been reported. There are four different mineral forms of titanium dioxide: rutile, brookite, anatase, and titanium dioxide (B). The crystal structure of anatase type TiO_2 corresponds to the quaternary system, which is primarily employed as a photocatalyst when exposed to UV light. The crystal structure of rutile TiO_2 is tetragonal in shape. It is frequently utilised in paint as a white pigment. The Brookite kind of TiO_2, on the other hand, has a distinct crystal structure. Within the titania family, titanium dioxide (B) is a relatively recent type of monoclinic metal. TiO_2 photocatalysis is appealing because it offers a renewable energy source based on solar energy. Furthermore, the material can be readily obtained due to its stable chemical structure, biocompatibility, and favourable physical, optical, and electrical properties. Since titanium is the ninth most prevalent element and the seventh most abundant metal in the world, titanium dioxide is a cheap material4. For applications involving the treatment of wastewater, titanium dioxide can be employed as a fine powder or as scattered crystals. A semiconductor is made of titanium dioxide. The UV (near ultraviolet) light with a wavelength of can activate these semiconductors. Indigo dye photodegradation utilising a TiO_2/zeolite 8403 combination. 3,90 nm 4,10. Electron (e^-) hole (h^+) pairs are created when UV light is applied to TiO_2 **(**Alhattab S & Johnson., 2021). The electron-hole pairs that are produced have the ability to start redox reactions on the surface of TiO_2 particles (El-Sayed B. A, 2019).. In an aqueous solution, surface hydroxyl groups scavenge holes to create active oxidative hydroxyl radicals (•OH). Subsequently, the organic substrate will fully mineralize as a result of the reactive hydroxyl radicals' quick reaction with organic molecules (Tianzhi .W 2021 & Srivastava. A. R., 2022) **.**However, TiO_2 is grafted with other materials like iron, activated carbon, or zeolite to improve its qualities, such as improving its adsorption capabilities or facilitating the quick separation of the photocatalyst from the treated solution**(**Vaez Z. 2020, Liu X., 2018**).** Zeolite is a solid crystal with a three-dimensional crystalline structure resembling a honeycomb made of interconnecting tubes and cages. These pores allow water to pass through freely, but the zeolite structure doesn't bend **(**Wu L.-P.,2009). Zeolite can function as a molecular sieve because its pore and channel diameters are almost consistent. Zeolite's special porous quality enables it to function as an absorbent in separation processes (Guo W., et al 2018). Cation exchange is one of zeolite's additional abilities. Zeolites' consistent pore and channel sizes, strong adsorption capacity, and regular pore and channel sizes make them a potential substrate for TiO_2 photocatalys (El-Mekkawi D.M.,2020) TiO_2 supported on zeolite produces a synergistic impact by combining the photocatalytic activity of TiO_2 with the adsorption capabilities of zeolite. An increase in photocatalytic efficiency is the consequence of this impact. Stated differently, the TiO_2 supported by zeolite has a higher surface area and is more uniformly diffused towards it, allowing for better adsorption and degradation 6 (Alhattab.s, Jamil, F & Rashad, M.A. et al., 2021). Because of their hydrophilicity, zeolites are also perfect supports for TiO_2. (Behravesh S.,2020). This investigation has also continuously evaluated the sample's recyclable quality and its capacity to function as an active photocatalyst during daylight hours in the mineralization of commercial industrial wastewater. Moreover, the photodegradation process of Blue Dianix dye was impacted by Zeolite-TQD catalyst as a distinct photocatalyst

(Barberio M., 2015).

Materials and Methods

Materials and reagents

All chemicals used throughout the work, are analytical grade and used without further purification., We bought 99.5% isopropanol and titanium (IV) isopropoxide (TTIP) from Fisher Company. The Fluka Company provided the commercial powder cetyl trimethyl ammonium bromide (CTAB), and de-ionized water was used. Ethanol 99.8% Fisher Company. HNO_3 nitric acid Fluka Company Commercial powder Zeolite.

Apparatus

Using a Philips XL-30 SEM analyzer (JEOL – JSM – T330 A) with an acceleration voltage of 30 KV, scanning electron microscopy (SEM) of MWCNTs and MWCNTs/x% Zeolite-TQD nanocomposites was observed .Using a Philips Holland device, X-ray diffraction images were obtained. Xpert MPD model with Cu-Kα target. (Data acquired with a step size of 0.017° and 100 s/step; Cu Kα radiation = 0.154 nm, 40 mA, 50 keV) . Xpert MPD model with Cu-Kα target. (Data acquired with a step size of 0.017° and 100 s/step; Cu Kα radiation = 0.154 nm, 40 mA, 50 keV).
JASCO IR-410 spectrometer (Germany) was used to measure IR spectra in the 4000-400 cm-1 region. Japanese instrument JASCO UV/VIS Spectrometer V-630 was used for all absorbance measurements. A JENWAY 3510 pH metre (UK) was used to measure each pH value. An electronic balance SHIMADZU TW423L (Japan) was used for the weighing process. Using the Hanna COD Instrument, measure the chemical oxygen ratio (COD) based on the partitioning of chemicals dissolved or suspended in water.

Methods

Preparation of Titanium dioxide quantum dots samples

5.0 mL of TTIP was taken in a syringe and it was dissolved in 500 millilitres of isopropanol. For over ninety minutes, the combined mixture was agitated. 0.01 mole of aqueous CTAB was added drop-wise into the mixed solution. The resulting solution was stirred mechanically for about 24 h. until a white dry powder was obtained. This was removed from the beaker and transferred to the mortar for grinding. The finely ground sample was transferred into an alumina boat and calcinated at 330, 360, and 400 ºC for 30 min in a muffle furnace.

Preparation of Zeolite-TQD

TiO_2/Zeolite5 composites were made using sol-gel synthesis. Dropwise additions of 2 ml of C_2H_5OH and 4 ml of titanium butoxide were made. The solution was given the name A after about 30 minutes at room temperature and magnetic stirring. 0.4 ml of HNO_3 and 2 ml of H_2O were combined with 17 ml of C_2H_5OH. B was the mixture's label. Solution B was then added gradually while stirring at a rate of roughly 3 millilitres per minute. The procedure proceeds after a transparent solution has been produced after stirring for an hour at room temperature. The transparent solution was mixed for 30 minutes and then allowed to mature for 24 hours at room temperature after the addition of the necessary amount of zeolite that had been filtered through a 100 mesh screen.

Characterization

In the FTIR spectrum of Zeolite-TQD, the prominent band at 446 cm^{-1} is attributed to the symmetric bending vibration of Si(Al)-O (Thuadaij. P& Wu . P. L., 2009) .and the band observed at 545 cm^{-1} corresponds to the five-membered ring vibration (Wu. P. L & Liu. X., 2018). Another noteworthy absorption band appears at 786 cm^{-1} and indicates the symmetric stretching vibration of Si-O-Al (Liu.X & Ghouil B. et al., 2015). Other prominent bands appear in the spectrum at 1035 cm^{-1} and 1227 cm^{-1} related to the asymmetric stretching of Si-O-Si (Behravesh . S., 2020) Finally, the presence of hydroxide groups, OH, resulting from the adsorption of water molecules on the surface of the material was confirmed by the presence of a band at 1646 and 3660 cm^{-1}(Wu. P. L. 2018 & Piedra López. J. G, et L .,2021). In addition, the infrared spectra of titanium zeolite calcined at 500 °C are almost unchanged and are comparable to those of zeolite. (Felipe.B. H. S 2022) . Crystalline properties of the samples were examined by a PANalytical X-ray diffractometer). The particle shape and size of

the quantum dot samples were studied by a high-resolution transmission electron microscope (HRTEM), Philips/FEI BioTwin CM120. UVVis absorption spectra were measured on a Shimadzu UV260 spectrophotometer, Japan. Photoluminescence spectra were measured using a JASCO v-570 spectrophotometer, Rel-00, USA, and their apparent rate constant (kf) was calculated using the slope of fluorescence intensity versus illumination time curves. The specific surface area (SSA) as determined by the Brunauer-Emmett-Teller (BET) technique of the prepared catalysts was determined from the nitrogen adsorption isotherm at 77 K using a Tristar 3000 micrometer system, Micromeritics Instrument Corporation, USA, after degassing the prepared quantum dots. At 150°C for one hour. The specific surface area can be calculated using the following relationship:

$$S = \frac{6}{dx\rho} \quad (1)$$

where d is the average diameter of particles, q is the density of TiO_2, Zeolite-TQD are 4.230, 2.55 g/cm^{-3} respectively, and S is the BET-specific surface area **(**Madi. K et al., 2024**).** For the photodegradation processes, a photoreactor with a xenon lamp (Eng. Co., Ltd., Egypt) as a light source was used in the presence of water-a cooling cycle system to avoid the effect of the lamp temperature. Xenon lamp wavelength emits light from 200 to 1100 nm with a power intensity of 70 W/cm^2. In the presence of the photocatalyst samples, the mineralization of Blue Dianix dye and real wastewater (textile factory in Helwan city, Cairo, Egypt), was measured by a multi-parameter bench photometer. Chemical oxygen demand (COD) was determined with COD C99 Series Multiparameter Bench Photometers, Hanna, USA.

Results

Characterization

(*FTIR)*

Figure 1 represents the FTIR spectrum at various calcination temperature (25, 430, 460 and 500°C). The FT-IR analysis exposes distinctive spectrum absorption characteristics, In this study, zeolite and TiO_2 quantum dots (TQDs) with sizes ranging from 307 to 48 nm were prepared by the sol-gel method. In addition, one of the purposes of this study was the photocatalytic effect of Zeolite-TQD quantum dots (Zeolite-TQD) on the photodegradation of Blue Dianix dye(Mohamed W.A.A. W, Saad(2023**)**. The Zeolite-TQD composites were characterized using X-ray diffraction (XRD) and Fourier transform infrared (FTIR), providing insight into the diverse vibration modes exhibited by the functional groups. On the FTIR spectrum of **(**Liu X, 2018**).** Another noteworthy absorption band appears at 786 cm^{-1} and indicates the symmetric stretching vibration of Si-O-Al **(**Liu. X **.,** 2017 & Ghouil .B et al ., 2015 **).** Other prominent bands appear in the spectrum at 1035 cm^{-1} and 1227 cm^{-1} related to the asymmetric stretching of Si-O-Si **(**Behravesh.S, 2020**)** . Finally, the presence of hydroxide groups, OH, resulting from the adsorption of water molecules on the surface of the material was confirmed by the presence of a band at 1646 and 3660 cm^{-1} **(**Liu X., 2018 & Piedra . López**).** In addition, the IR spectra at 500 °C calcined remain almost unchanged and are comparable to those of Zeolite-TQD. With a mass of 20% TiO_2 according to XRD analysis. The Zeolite-TQD generated some small particles with multilayer structure, and the Zeolite-TQD particles aggregated and formed agglomerates, according to the SEM study. The rate of photodegradation of Blue Dianix dye in a xenon photoreactor in the presence of TQD reached $18.45\times10^{-3}S^{-1}$ and for Zeolite-TQD it reached $6.18\times10^{-3}S^{-1}$ while the maximum photodegradation reached 20%, 66% and 95% for Zeolite and Zeolite-TQD and TQD respectively (Mohamed W.A.A. W, Saad., 2023). The uniqueness of TQD in terms of crystal domain size is that it exhibits photocatalytic activity due to its large surface area and small size (less than 10 nm) (Zampino D ., 2011). We also used the COD limits stipulated in the Egyptian Environmental Law to verify the photodegradation rate of actual industrial effluents. Nine Zeolite-TQD samples were recycled and analyzed using COD measurements.

(*XRD)*

Figure 2 shows the XRD patterns of Zeolite,TQD,Zeolite-TQD. Several diffractions peaks appeared on the diffractograms at various angular positions 2θ= 8.08°, 13.27°, 15.9,

17.29°, 23.09°, could be attributed to the clinoptilolite type of natural zeolite according to JCPDS number of 25–1349 **(**Wu .P. , Wu L.-P **).** For TiO_2 the following angular positions 2θ= 25.62°, 37.31°, 47.38°, 54.76° and 62.27°. These peaks were assigned based on the pattern provided by the reference (JCPDS card No. 21-1272) as respectively (1 0 1), (0 0 4), (2 0 0), (1 0 5), (2 0 4) Bragg's planes of anatase structure (Liu X., 2018 & Almeida-Didry., 2016)). The average crystallite size (D) was calculated using Scherrer's equation (2) (Sabahi B. et al ., 2018).

$$D = \frac{k\lambda}{\beta \cos\theta} \quad (2)$$

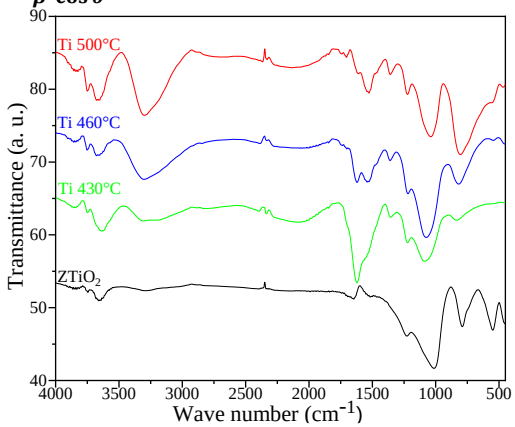

Figure 1 FTIR of Zeolite, TQD and Zeolite-TQD catalysts.

Indicating, k serves as a correction factor that accounts for particle shape, usually set at a value of 0.94. λ stands for the wavelength of the incident X-ray beam (approximately 1.5406 Å), while β represents the full width at half maximum (FWHM) of the diffraction peak, measured in radians. θ corresponds to half of Bragg's diffraction angle (Mohamed W.A.A. W, Saad(2023). The sample exhibited a crystal size on the scale of approximately 9.62 nm.

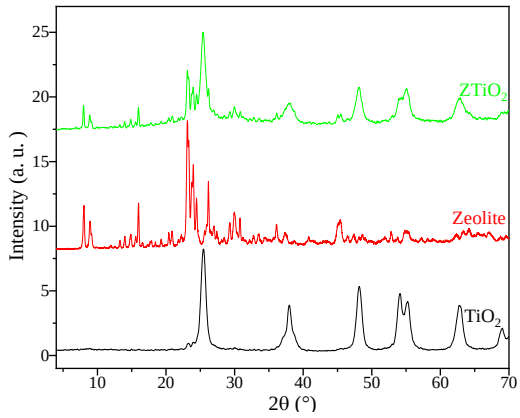

Figure 2 XRD of Zeolite, TQD and Zeolite-TQD catalysts.

SEM

The scanning electron microscopy (SEM) Figure 3 results predominantly reveal spherical TiO_2 particles in the TiO_2/zeolite samples observed at various magnifications of 50, 10, and 5 micrometers. This spherical morphology of TiO_2 particles is typical of the synthesis methods employed, indicating homogeneous and regular particle formation. However, some irregular grains are also observed, particularly in the image enlarged to 5 micrometers with a zoom of 3000. While this image is primarily intended for detailed particle visualization, the particle sizes appear fairly uniform, ranging from 1.7 to 2.6 micrometers (Álvarez1. M K., 2018). These size variations may be attributed to factors such as the initial distribution of TiO_2 particle sizes and the density of the zeolite layer. These observations provide valuable insights into particle morphology and TiO_2/zeolite interaction, with potential implications for catalytic applications of these materials.

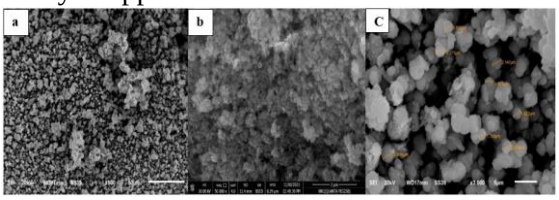

Figure 3 SEM of (a) Zeolite, (b) TQD and (c) Zeolite-TQD catalysts.

(*EDAX*)

Figure 4 EDAX analysis of Zeolite-TQD zeolite reveals a typical composition with a dominance of oxygen compared to zeolite (56.89% by mass, 73.53% by atoms), with the presence of a silicate and aluminate network. The presence of large amounts of silicon (19.16% by mass, 14.11% by atoms) and aluminum (3.02% by mass, 2.31% by atoms) confirm the typical crystal structure of Zeolite-TQD, while sodium (2.76% by mass, 2.48). % by atoms) suggests an exchange function. . Positive ions. Based on the results of elemental analysis using EDS spectroscopy, the surface of the TiO_2 modified Zeolite contains significant amounts of titanium (15.60% by mass, 6.74% by atoms). The presence of copper (1.50% by mass, 0.94% by atoms) and zinc (1.09% by mass, 0.34 atoms) also indicates % in atoms) indicates a modification in the substance that can enhance its catalytic properties or provide specific properties (Mohamed W.A.A. W, Saad., 2023).

In summary, the material appears to be a standard ZMS-TQD zeolite modified with Cu and Zn to provide photocatalytic analysis results of unmodified zeolite and Zeolite-TiO_2 using EDX. The chemical composition of zeolite includes O, Na, Al,. Si, Cu, Zn, symmetric substitution of metal cations **(**El-Sayed B. A., 2019 **).** The zeolite-TiO_2 photocatalyst shows the following spectrum O, Na, Al, Si, Cu, Zn, and Ti Using the EDS spectrum, the surface of the modified zeolite contains more TiO_2 than the pure zeolite, which is shown in Figure 4.

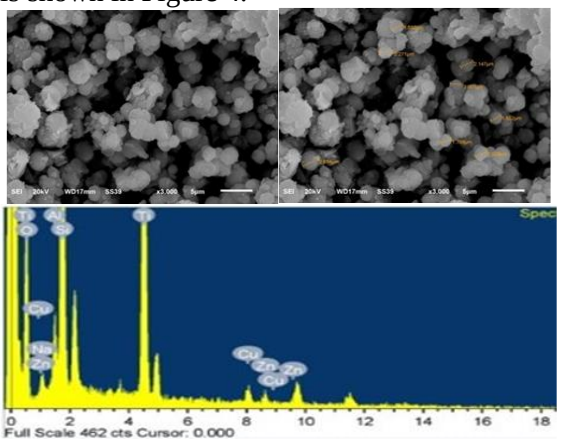

Figure 4 EDX of Zeolite-TQD catalysts at different zoom.

TEM

Transmission electron microscopy (TEM) data reveal distinct differences between zeolite (ZMS5)alone and the composite Zeolite-TQD (TiO_2/Zeolite5). For zeolite (ZMS5) Figure 5(a)and (b), TEM images show a variety of particle sizes ranging from 307 to 48 nm, as well as a mix of spherical and rectangular shapes. This diversity in size and shape suggests variations in growth mechanisms or crystalline structure, which could potentially influence the physical and chemical properties of the zeolite **(**Fernańdez - Catala ., 2017). Despite the broad distribution of sizes, it remains relatively homogeneous, which may positively impact specific surface area, adsorption capabilities, and catalytic performance. In contrast, TEM images of Zeolite-TQD show a narrower range of particle sizes from 3.83 to 7.01 nm, with uniform spherical shapes. This tight distribution of sizes and consistent shape suggests an even dispersion of TiO_2 within the zeolite matrix (Kanakaraju D., 2015). This results in an increase in specific surface area and better composite dispersion, thereby enhancing its catalytic and adsorption properties. In summary, zeolite ZMS5 alone presents a wide range of particle sizes (Nejad-Darzi (2013) and shapes, which can variably influence its physical

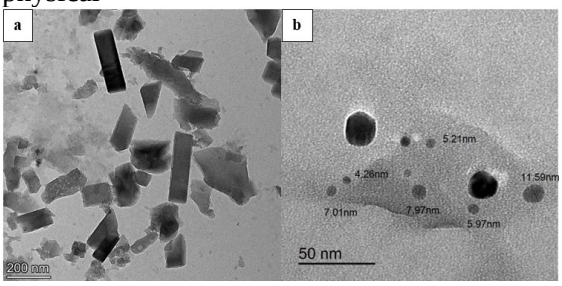

Figure 5 TEM of(a) Zeolite5 and (b)Zeolite-TQD composite.

and chemical properties. Conversely, the composite Zeolite-TQD offers a more uniform distribution of small spherical particles, potentially strengthening its performance in applications requiring high specific surface area and efficient interaction with reactants which is shown in Figure. 5

Bandgap

The bandgap energy of ZMS5 was determined using Tauc's plot and found to be 3.92 eV, suggesting that ZMS5 is a material with a relatively large bandgap.

For the Zeolite-TQD sample, which is a composite material containing zeolite modified with TiO_2, the UV absorption is also pronounced. A distinct absorption peak was observed around 294 nm, similar to ZMS5 but slightly shifted. The determination of the bandgap energy for Zeolite-TQD shows a value of 3.57 eV, which is lower than that of ZMS5. Comparing the two samples reveals that incorporating TiO_2 into the zeolite (to form Zeolite-TQD) leads to a slight reduction in the bandgap energy, from 3.92 eV to 3.57 eV. This could be due to the effect of TiO_2 on the overall electronic structure of the zeolite, causing a modification of the energy levels of the valence and conduction bands. By reducing the bandgap, Zeolite-TQD may have better potential for absorbing visible light compared to ZMS5, which can be advantageous for photocatalytic or optical applications.

Furthermore, the BET surface areas of Zeolite - TQD are 292.39 m^2/g, respectively. The strong photocatalytic activity of the Zeolite-TQD photocatalyst (high surface area and a distinct crystalline domain size of less than 10 nm)

causes it to degrade quickly.

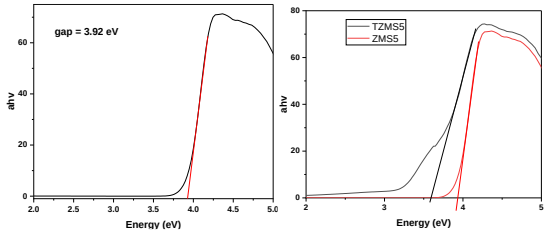

(a) (b)

Figure 6. Tauc`s plot, bandgaps and Diffuse reflectance of (a) Zeolite, (b)Zeolite -TQD

Discussion

Photocatalytic efficiency blue Dianix dye of Zeolite -TQD

Using a Xenon photoreactor (70 watts/cm^2 and a wavelength range of 200-1050 nm), the following photocatalytic technique can be performed to test photocatalytic efficacy and improve photodegradation of Blue Dianix dye is an industrial product.100 ml of dye solution (2×10^{-5} M, pH = 7) with 0.1 g of Zeolite-TQD dispersed evenly (El-Sayed B. A., 2019) .To test the adsorption and desorption equilibrium, TiO_2 was added to the dye and mixed in the dark for 15 minutes. The Thermo MEGAFUGE 16 must be immediately centrifuged for 20 minutes at 10,000 rpm to recover any last bits of catalyst from the suspension.As shown in Figure. 7, the rates of photodegradation for each photodegradation process using xenon photoreactors and sunlight photocatalytic for Dianix blue dye in the presence of Zeolite-TQD samples. The kinetic curve for each photodegradation process is shown in Fig. 6 and demonstrates a linear relationship between (ln (C_0/C) and irradiation duration). Furthermore, as previously demonstrated (Zare ., 2022), the fundamental mechanism for the photodegradation of blue Dianix dye is the formation of hydroxyl radicals. The proposed mechanisms for the photodegradation of blue Dianix dye in the presence of prepared catalysts when the catalyst is exposed to a light source include the transfer of excited electrons (e^-) to a higher level and the production of a positive hole (h^+) at the lower level of the preceding level. Consequently, Superoxide is the reactive species that was detected. Additionally, as was previously shown (Zare., 2022), the production of hydroxyl radicals is the primary mechanism underlying the photodegradation of the blue Dianix dye. Based on the interaction of (O_2) and (H_2O) molecules with e- and h+ radicals, respectively, the proposed blue Dianix dye process is described(Takeuchi, M., 2007) & Takeuchi, M., 2012). Following that, the degradation was finished by focusing on the blue Dianix dye molecule's active species (Felipe B. H. S., 2017) . According to the mechanism described above for the photodegradation of blue Dianix dye by TQDs initials in the valence band region, when the produced photocatalysts (TQDs) are exposed to radiation, the electrons will be transferred from the valence band region to the conduction band region. The valence band region is where this process starts, and the conduction band region is where it ends. Next, a positive hole (h^+) was created at a lower energy level while just one electron moved to a higher energy level of the excited negative electron (e^-) (Mohamed W.A.A. W, Saad ., 2023). Thus, it is possible to think of these two procedures as byproducts of the photocatalysis process. The generation of hydroxyl radicals is the primary mechanism by which photodegradation of Dianix blue dye occurs (Mohamed W. A. A ., 2019). The catalyst produced (h^+) at a lower level and the excited electrons (e^-) migrated to a higher level when exposed to a light source. Providing evidence for the photodegradation of Blue Dianix in the presence of Zeolite-TQD catalysts. The reactive species that can be detected are therefore superoxides, and the production of hydroxyl radicals is essential for the photodegradation of Blue Dianix dye. When water and oxygen dioxide come into contact with the (e^-) and (h^+) radicals, Blue Dianix decomposes. The active species of Dianix blue dye was the center of attention to complete the decomposition process. (Al-Hattab S ,2022) furthermore, the general photocatalytic mechanism step is investigated as follows for Zeolite -TQD : shown in scheme 1.

$$\text{Zeolite} - TiO_2 + h\nu(UV) \rightarrow \text{Zeolite}(e^-)(CB) + \text{Zeolite} - TiO_2(h^+)(VB) \quad (3)$$

$$h^+ + H_2O \rightarrow {}^{\cdot}OH + H^+ \quad (4)$$

$$e^- + O_2 \rightarrow O_2^{\cdot-} \quad (5)$$

$$H_2O + O_2^{\cdot-} \rightarrow HO_2^{\cdot} + {}^{\cdot}OH \quad (6)$$

$$2HO_2^{\cdot} \rightarrow H_2O_2 + O_2 \quad (7)$$

$$H_2O_2 + O_2^{\cdot} \rightarrow {}^{\cdot}OH + OH^- + O_2 \quad (8)$$

$$\text{Dye} + {}^{\cdot}OH + O_2^{\cdot-} \rightarrow \text{Degraded organic dye} \quad (9)$$

$$\text{Degraded organic dye} + {}^{\cdot}OH^{\cdot} + O_2^{-} \rightarrow H_2O + CO_2 \quad (10)$$

Scheme 1. The suggested mechanism for photodegradation of Blue Dianix dye in presence of Zeolite -TQD

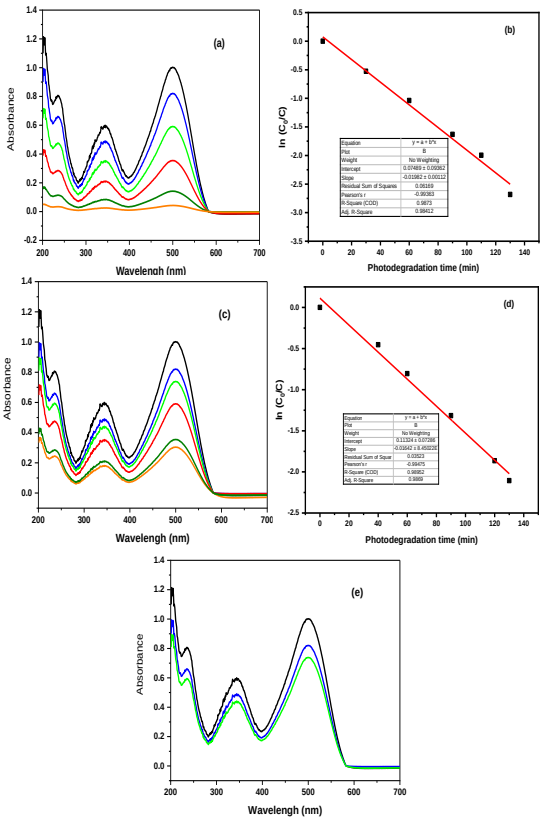

Figure 7. Absorption spectra and Blue dye photodegradation rate kinetics plot

Dianix in presence of (a, b) TiO_2QD, (c,d) zeolite/TiO_2QD, (e) zeolite by xenon photoreactor.

The electrons in zeolite TQDs can be excited to move from the valence to the conduction band. In zeolite- TQD, electrons can move from valence to conduction bands when exposed to light. A positively charged hole is created in the valence band of a substance when an electron leaves. The electron-hole pairs will combine quickly if they do not reach the top of the Zeolite-TQD nanostructures. The electron-hole pairs on the surfaces of the Zeolite-TQD nanostructure can interact with water, oxygen, and other materials. Some of these compounds can be reduced through electron donation, whereas others are oxidized by holes. Photocatalysis can be used to produce a wide range of products, including hydrogen gas and clean water. The Blue Dianix dye's rate of photodegradation in presence of TQD = 18.45×10^{-3} S^{-1} and with Zeolite-TQD =8.45×10^{-3} S^{-1}. The findings suggest that, the photocatalytic efficiency improves by adding of TQD as in Zeolite -TQD composite. These results show that the quantum size effect of TQD photocatalysts influences on the photocatalytic efficacy of Zeolite-TQD compared to Zeolite catalyst (without TiO_2).

Recycling processes

Commercial industrial wastewater with a pH in the range of 7.0 is subjected to the photocatalysis process, it is treated in direct sunshine with 4.1 mW/cm^2 UV and 1078 mW/ cm^2 visible light. The following mineralization equation

$$\text{Mineralization \%} = 100x[(COD)_0 - (COD)_t]/(COD)_0 \quad (11)$$

was used to assess the photocatalytic activity of each sample at time t

where the COD values are COD_0 and COD_t, respectively, at time 0 and time t. Depending on how the chemicals break down chemically in suspended or dissolved water, a COD Hanna spectrophotometer is used. Six estimations and validations of the Zeolite-TQD photocatalyst recycling method were performed. via spectrophotometry method. According to Chemical Oxygen Demand (COD) and as an estimate approach, the greatest percentage of all photocatalytic activity was measured. As can be seen in Figure 8, the obtained data indicate that the size accumulation of Zeolite-TQD leads to size increase during photodegradation by sunlight due to the thermal processes accompanying the light. The duration of sunlight irradiation was nine hours. Figure 8. This observation is related to the long duration of solar radiation, up to nine hours, as well as the increased size of TQDs due to accretion and slowing of photodecomposition.

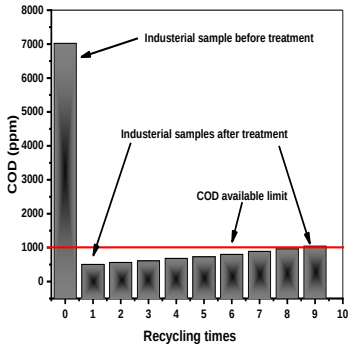

Figure 8. COD values for an industrial sample under solar radiation during the Zeolite-TQD sample recycling process.

Conclusion

In our study, Zeolite-TQD shows anatase phases structure form zeolite-TQD, while SEM-EDX data reveal that zeolite-TQD produces a large number of small particles with a multilayer structure. The Zeolite-TQD, which has an average diameter of 52.67 nm, It was subjected to calcination for five hours at 500°C using a wet chemical technique. Each Zeolite-TQD sample shows excellent single-step purity as measured by XRD and TEM. In addition, in the presence of Zeolite-TQD, the photodegradation rate of Blue Dianix dye reaches a detectable value of $8.54\times10^{-3}S^{-1}$, while no noticeable degradation of zeolite was detected in the absence of TiO_2. As in the case of the Zeolite-TQD complex, the results indicate that the addition of TQD increases the photocatalytic efficiency. These results demonstrate that compared with the zeolite catalyst (without TiO_2), the photocatalytic efficiency of zeolite-TQD is affected by the TQD photocatalysts' quantum size influence The results of the COD investigation finally confirmed the previous observation that photodegradation reached a significant rate with 9 recycling processes (Piedra J.G ., 2021). The results of this study led to recent contributions of Zeolite-TQD, which, due to its special size effect and optical tunability properties associated with its structures, serves as an excellent photocatalyst in many cutting-edge applications.

References

Ahsan, A., Jamil, F., Rashad, M.A. et al. Wastewater from the textile industry: Review of the technologies for wastewater treatment and reuse. Korean J. Chem. Eng. 40, 206 02081(2023).https://doi.org/10.1007/s11814-023-1475-2

Almeida-Didry S. de, C. Autret, C. Honstettre, A. Lucas, M. Zaghrioui, F. Pacreau and F. Gervais., Central role of TiO2 anatase grain boundaries on resistivity of CaCu3Ti4O12-based materials probed by Raman spectroscopy. Solid State Sciences 61 (2016) p.p. 102-105.https://doi.org/10.1016/j.solidstatesciences.2016.07.010

Alhattab S. and Johnson C.. (2021) 'Billions of people will lack access to safe water, sanitation and hygiene in 2030 unless progress quadruples – warn WHO, UNICEF', [viewed 2022 May 2022]; Available from: https://www.unicef.org/press-releases/billions-people-will-lack-access-safe-water-sanitation-and-hygiene-2030-unless

Arveen.S, Paul K.K., Das R, Giri, Giri P.K., Large exciton binding energy, high photoluminescence quantum yield and improved photostability of organo-metal halide hybrid perovskite quantum dots grown on a mesoporous titanium dioxide template, J Colloid Interface Sci 539 (2019) 619-633.

B.H.S. Felipe, Cabral R.L.B, Ladchumananandasivam R, Zille A, Kim S, Fechine P.B.A, Nascimento J.H.O., Nanocoating on cotton fabric with nitrogen-doped graphene quantum dots/titanium dioxide/PVA: an erythemal UV protection and photoluminescent finishing, Journal of Materials Research and Technology 18 (2022) 2435-2450.

Bajuk-Bogdanović D, Popa A, Uskoković-Marković S., et I. Holclajtner-Antunović, « Vibrational study of interaction between 12-tungstophosphoric acid and microporous/mesoporous supports », Vib. Spectrosc., vol. 92, p. 151-161, sept. 2017, doi: 10.1016/j.vibspec.2017.06.007.

Barberio M, Stranges F, Imbrogno A, Xu F., Growth of core-shell quantum dots/titanium dioxide hybrid films as photoanode for Graetzel cells, Surface and Coatings Technology 271 (2015) 259-264.

Behravesh S, Mirghaffar N, Alemrajabi A. A, Davar F,et Soleimani M., « Photocatalytic degradation of acetaminophen and codeine medicines using a novel zeolite-supported TiO2 and ZnO under UV and sunlight irradiation », Environ. Sci. Pollut. Res., vol. 27, no 21, p. 26929-26942, juill. 2020, doi: 10.1007/s11356-020-09038- Nivoix Y. x, Ledoux M.P, Herbrecht R. Herbrecht, Antifungal Therapy: New and Evolving Therapies, Semin Respir Crit Care Med 41(1) (2020) 158-174.

Berekaa M.M., Nanotechnology in Wastewater Treatment; Influence of Nanomaterials on Microbial Systems, International Journal of Current Microbiology and Applied Sciences 5(1) (2016) 713-726.

de Oliveira C.R.S, de Oliveira P.V, Pellenz. L, de Aguiar C.R.L. de Aguiar, A.H. da Silva Junior, Supercritical fluid technology as a sustainable alternative method for textile dyeing: An approach on waste, energy, and CO2 emission reduction, Journal of Environmental Sciences 140 (2024) 123-145.

El-Mekkawi D.M, Abdelwahab N.A, Mohamed W.A.A, Taha N.A, Abdel-Mottaleb, M.S.A., Solar photocatalytic treatment of industrial wastewater utilizing recycled polymeric disposals as TiO2 supports, Journal of Cleaner

Production 249 (2020) 119430.

El-Sayed B. A., Mohamed. W. A. A, Galal H. R., Abd El-Bary H. M., and Ahmed M. A. M. (2019). Egyptian Journal of Petroleum. 28(2), 247-252.

Felipe B. H. S, Cabral R. , Ladchumananandasivam L. B, Zille.R, Kim A, S, Fechine. P. B. A. and Nascimento J. H. O. Nascimento. (2022). Journal of Materials Research and Technology. 18, 2435-2450.

Fernańdez-Catala,́J.;Cano-Casanova,L.;Lillo-Roḑenas,M.A.;Berenguer-Murcia,Á.;Cazorla Amoroś,D.Synthesis of TiO2 with hierarchical porosity for the photooxidation of propene. Molecules 2017, 22, No. 2243.

Ghoui.B. et al., « Development and characterization of tubular composite ceramic membranes using natural alumino-silicates for microfiltration applications », Mater. Charact., vol. 103, p. 18-27, mai 2015.

Ghouil B, Harabi .A, Bouzerara F., B. Boudaira, Guechi A, Demir M.M, Figol A., Development and characterization of tubular composite ceramic membranes using natural alumino-silicates for microfiltration applications, Materials Characterization 103 (2015) 18-27.

Irirerkratana.K, Kemacheevakul .P. l, Chuangchot.S., Color removal from wastewater by photocatalytic process using titanium dioxide-coated glass, ceramic tile, and stainless steel sheets, Journal of Cleaner Production 215 (2019) 123-130.

Joksimovic K. c, Kodranov, I, Randjelovic D., Beskoski Slavkovic L, Radulovic J, Ljesevic M., D. Manojlovic, Beskoski V.P. i, Microbial fuel cells as an electrical energy source for degradation followed by decolorization of Reactive Black 5 azo dye, Bioelectrochemistry 145 (2022) 108088.

Kozak M, Cirik K, Başak S., Treatment of textile wastewater using combined anaerobic moving bed biofilm reactor and powdered activated carbon-aerobic membrane reactor, Journal of Environmental Chemical Engineering 9(4) (2021) 105596.

Kanakaraju D., Kockler, J. Motti C.A. Motti, Glass B.D. Glass, M. Oelgemoller, Titanium dioxide/zeolite integrated photocatalytic adsorbents for the degradation of amoxicillin,Appl.Catal.B-Environ.166-167(2015) 45-55

Lanjwani M.F, Tuzen M, Khuhawar M.Y, Saleh T.A,Trends in photocatalytic degradation of organic dye pollutants using nanoparticles: A review, Inorganic Chemistry Communications 159 (2024) 111613.

Liu X., Liu Y, Lu S., Guo W., et Xi B.,« Performance and mechanism into TiO2/Zeolite composites for sulfadiazine adsorption and photodegradation », Chem. Eng. J., vol. 350, p. 131-147, oct. 2018, doi: 10.1016/j.cej.2018.05.141.

Madi K. i et al., « Green Fabrication of ZnO Nanoparticles and ZnO/rGO Nanocomposites from Algerian Date Syrup Extract: Synthesis, Characterization, and Augmented Photocatalytic Efficiency in Methylene Blue Degradation », Catalysts, vol. 14, no 1, p. 62, janv. 2024, doi: 10.3390/catal14010062.

Mohamed W, El-Gawad H.A, Handal H., Galal H. l, Mousa H. El-Sayed Mousa, B, Mekkey S., brahem I., Labib A. Labib, Remarkable Recycling Process of ZnO Quantum Dots for Photodegradation of Reactive Yellow Dye and Solar Photocatalytic Treatment Process of Industrial Wastewater, Nanomaterials (Basel) 12(15) (2022) 2642.

Mohamed W, El-Gawad H.A, Handal H., Galal H. l, Mousa H. El-Sayed Mousa, B, Mekkey S., brahem .I. , Labib A. Labib,, TiO2 quantum dots: Energy consumption cost,germination, and phytotoxicity studies, recycling photo and solar catalytic processes of reactive yellow 145 dye and natural industrial wastewater, Advanced Powder Technology 34(1) (2023) 103923.

Mohamed W.A.A. W, Saad.M. W, F.S. Mohamed, A.A. El-Bindary, Distinguishable Recycling and Photodegradation Processes of Real Industrial Effluents and Blue Dianix Dye in the Presence of Different TQDs Size, Journal of Cluster Science 35(2) (2023) 575-584

Mojgan Zendehdel • Akbar Zendehnam • Fatemeh Hoseini • Mohammad Azarkish Investigation of removal of chemical oxygen demand (COD) wastewater and antibacterial activity of nanosilver incorporated in poly (acrylamide-co- acrylic acid)/NaY zeolite nanocomposite Polym. Bull. (2015) 72:1281–1300

Nejad-Darzi, H.; Samadi-Maybodi, A.; Ghobakhluo, M. Synthesis and characterization of modified ZSM5 nanozeolite and their applications in adsorption of Acridine Orange dye from aqueous solution. J. Porous Mater. 20, 909−916.

Naswir M, Arita S., Marsi, Salni, Characterization of Bentonite by XRD and SEM-EDS and Use to Increase PH and Color Removal, Fe and Organic Substances in Peat Water, Journal of Clean Energy Technologies (2013) 313-317.

Nivoix Y., Ledoux M.P, Herbrecht R., Antifungal Therapy: New and Evolving Therapies, Semin Respir Crit Care Med 41(1) (2020) 158-174.

Piedra J.G. López, Pichardo .González O.H, Pinedo Escobar , Escobar. Pinedo J.A, D.A. de Haro del Río, H. Inchaurregui Méndez, L.M. González Rodríguez, Photocatalytic degradation of metoprolol in aqueous medium using a

TiO2/natural zeolite composite, Fuel 284 (2021) 119030.

Rahmani-Aliabadi A. et A. Nezamzadeh-Ejhieh, « A visible light FeS/Fe 2 S 3 /zeolite photocatalyst towards photodegradation of ciprofloxacin », J. Photochem. Photobiol. Chem., vol. 357, p. 1-10, avr. 2018

Ramesh K., Gnanamangai B.M. , Mohanraj R., Investigating techno-economic feasibility of biologically pretreated textile wastewater treatment by electrochemical oxidation process towards zero sludge concept, Journal of Environmental Chemical Engineering 9(5) (2021) 106289.

Sabahi H, Khorami M, Rezayan A.H, Jafari Y, Karami M.H., Surface functionalization of halloysite nanotubes via curcumin inclusion, Colloids and Surfaces A: Physicochemical and Engineering Aspects 538 (2018) 834-840.

Shakiba Mohammadhosseini 1, Tariq J. Al-Musawi 2, Rosario Mireya Romero Parra 3, Mutaz Qutob4, M. Abdulfadhil Gatea 5, Fatemeh Ganji 6 and Davoud Balarak 7,*Nanocomposite.Minerals 2022, 12, 1417. https://doi.org/10.3390/ min12111417

Suhan M.B.K, Al-Mamun M.R, Farzana N., S.M. Aishee, Islam M.S, Marwan.H.M, Hasan M.M, AsirA.M., Rahman M.M, Islam A., Awual M.R, Sustainable pollutant removal and wastewater remediation using TiO2-based nanocomposites: A critical review, Nano-Structures & Nano-Objects 36 (2023) 101050.

Taylo M., Pullar R.C, Parkin I.P, Piccirillo. C., Nanostructured titanium dioxide coatings prepared by Aerosol Assisted Chemical Vapour Deposition (AACVD), Journal of Photochemistry and Photobiology A: Chemistry 400 (2020) 112727.

Thuadaij P, Nuntiy A., Preparation and Characterization of Faujasite using Fly Ash and Amorphous Silica from Rice Husk Ash, Procedia Engineering 32 (2012) 1026-1032.

Vae Z, avanbakht V., Synthesis, characterization and photocatalytic activity of ZSM-5/ZnO nanocomposite modified by Ag nanoparticles for methyl orange degradation, Journal of Photochemistry and Photobiology A: Chemistry 388 (2020) 112064.

Takeuchi, M.; Kimura, T.; Hidaka, M.; Rakhmawaty, D.; Anpo, M. Photocatalytic oxidation of acetaldehyde with oxygen on TiO2/ ZSM5 photocatalysts: Effect of hydrophobicity of zeolites. J. Catal. 2007, 246, 235−240.

Takeuchi, M.; Hidaka, M.; Anpo, M. Efficient removal of toluene and benzene in gas phase by the TiO2/Y-zeolite hybrid photocatalyst. J. Hazard. Mater. 2012, 237, 133−139

Wu J, Zhang .D, Cao Y. Fabrication of iron-doped titanium dioxide quantum dots/molybdenum disulfide nanoflower for ethanol gas sensing, J Colloid Interface Sci 529 (2018) 556-567.

Wu K,Zhang W, Zheng Z, Debliquy M., and Zhang C. (2022) Applied Surface Science. 585, 152744.

Wu L.-P, Li. X.-J, Yuan Z.-H., Chen Y., The fabrication of TiO2-supported zeolite with core/shell heterostructure for ethanol dehydration to ethylene, Catalysis Communications 11(1) (2009) 67-70.

Yen Y. C, Lin C. C., Chen P. Y, Ko W. Y, Tien T. R., and Lin K. J.. (2017). R Soc Open Sci. 4(5), 161051.

Zare A. Shenavaie, Ganjeali A, Vaezi Kakhki M. R, Mashreghi. M., and Cheniany M. 2023.. 25, 100659.

Zampino D, Ferreri T, Puglisi C, Mancuso M, Zaccone R, Scaffaro R, Bernardo D 2011 PVC silver zeolite composites with antimicrobial properties. J Mater Sci 46:6734–6743.

.

الملخص العربي

عنوان البحث: عمليات التحلل الضوئي لمياه الصرف الصناعي التجاري وصبغة Blue Dianix في وجود Zeolite-TQD

وليد م. سعد[١]، فريد ش. محمد[١]، أشرف أ. البنداري[١] وليد أ.أ. محمد*[٢]

[١]قسم الكيمياء، كلية العلوم، جامعة دمياط، دمياط ٣٤٥١٧، مصر.
[٢] قسم الكيمياء غير العضوية، المركز القومي للبحوث، الدقي، الجيزة، مصر.

في دراستنا، يُظهر Zeolite-TQD بنية مراحل الأناتاز من الزيوليت-TQD، بينما تكشف بيانات SEM-EDX أن الزيوليت-TQD ينتج عددًا كبيرًا من الجزيئات الصغيرة ذات بنية متعددة الطبقات. تم تعريض الزيوليت-TQD، الذي يبلغ متوسط قطره

٥٢,٦٧ نانومتر، للتكلس لمدة خمس ساعات عند درجة حرارة ٥٠٠ درجة مئوية باستخدام تقنية كيميائية رطبة. تُظهر كل عينة Zeolite-TQD درجة نقاء ممتازة في خطوة واحدة كما تم قياسها بواسطة XRD وTEM. بالإضافة إلى ذلك، في وجود Zeolite-TQD، يصل معدل التحلل الضوئي لصبغة Blue Dianix إلى قيمة يمكن اكتشافها تبلغ 8.45×10^{-3} S^{-1}، في حين لم يتم اكتشاف أي تحلل ملحوظ للزيوليت في غياب TiO_2. كما في حالة مجمع Zeolite-TQD، تشير النتائج إلى أن إضافة TQD يزيد من كفاءة التحفيز الضوئي. توضح هذه النتائج أنه بالمقارنة مع محفز الزيوليت (بدون TiO_2)، تتأثر كفاءة التحفيز الضوئي للزيوليت-TQD بتأثير الحجم الكمي لمحفزات TQD الضوئية. وأكدت نتائج تحقيق COD أخيرًا الملاحظة السابقة التي مفادها أن التحلل الضوئي وصل إلى معدل كبير مع ٩ عمليات إعادة التدوير (Piedra J.G., 2021). أدت نتائج هذه الدراسة إلى مساهمات حديثة لـ Zeolite-TQD، والذي، نظرًا لتأثير حجمه الخاص وخصائص الضبط البصري المرتبطة بهياكله، يعمل كمحفز ضوئي ممتاز في العديد من التطبيقات المتطورة.